RSC Advances

ROYAL SOCIETY OF CHEMISTRY

www.rsc.org/advances

Cite this: DOI: 10.1039/c0xx00000x

www.rsc.org/xxxxxx

ARTICLE TYPE

Enhanced visible light photocatalytic activity of polyaniline-crystalline TiO_2-halloysite composite nanotubes by tuning the acid dopant in the preparation

Cuiping Li,* Tianzhu Zhou, Tianwen Zhu and Xueyuan Li

Received (in XXX, XXX) Xth XXXXXXXXX 20XX, Accepted Xth XXXXXXXXX 20XX
DOI: 10.1039/b000000x

Tubular halloysite minerals are used as support for the fabrication of one-dimensional polyaniline-crystalline TiO_2-halloysite composite nanotubes in the presence of different acid dopant at low temperature. By simply adjusting the acidity of reaction system, PANI-crystalline TiO_2-HA composite nanotubes composed of anatase, a mixed phase TiO_2 and different PANI redox state are obtained. The acidity of reaction system is tuned by HNO_3, HCl, H_2SO_4 and H_3PO_4, respectively. The traditional thermal treatment for crystalline transformation is not required, thus intact halloysite structure can be guaranteed. The XRD and UV-vis results show that the surface polyaniline sensitization has no effect on the crystalline structure of halloysite and the light response of TiO_2 is extended to visible-light regions, respectively. The visible light photocatalytic activity of polyaniline-crystalline TiO_2-halloysite with HCl tuning the acidity (pH 0.5) and 1% volume ratio of aniline to titanium isopropoxide in the preparation (P-TH/0.5/1%-HCl) is superior to those of samples with H_2SO_4, HNO_3 and H_3PO_4 tuning the acidity in the preparation at the same acidity and volume ratio of aniline to titanium isopropoxide. Such superior photocatalytic activity of P-TH/0.5/1%-HCl is mainly due to the enhanced visible light adsorption and electrical conductivity. Furthermore, redoping P-TH/0.5/1%-HCl with H_2SO_4 and H_3PO_4 demonstrates its photocatalytic activity is decreased, indicating the acid dopant in the preparation and redoping process play a important role to the photocatalytic activity of the polyaniline-crystalline TiO_2-halloysite composite nanotubes. Moreover, the supported catalyst allows them to be easily separated from the solution.

1. Introduction

During the past decades, clay mineral supported catalysts with high efficiency have been widely studied for potential application in air purification and photocatalytic degradation of organic pollutants, owing to their large surface area, high cation exchange capacity and the excellent enrichment ability for organic reactants either on their external surfaces or within their interplanar spaces by intercalation or substitution.[1-6] Among the clay mineral families, tubular halloysite (a chemical formula of $Al_2Si_2O_5(OH)_4.2H_2O$) which is similar to kaolinite except for the presence of an additional water monolayer between the adjacent clay layers, has garnered particular interests due to its versatile features of large surface area, high porosity, and tunable surface chemistry, which enabled this nanomaterial to be utilized as an attractive support for the assembly of small-size metals and metal-oxide and hydroxide aggregates (clusters and nanoparticles).[7-11] Furthermore, the clay nanotubes possess the advantages of high stability, resistibility against organic solvents, and ease of disposal or reusability as well.[12] Compared to carbon nanotubes, they are economically available natural materials and have many unique characteristics including different outside/inside chemical properties and adequate hydroxyl groups on the surface.[10,12] These groups can react with organochlorosilanes and alkoxides giving covalently bonded organic-inorganic derivatives,[13-17] which is useful for anchoring catalyst particles on the halloysite surface. Recently, various catalyst compounds (ATRP catalyst, silver and ruthenium) loaded on the tubular halloysite mineral have been reported with excellent catalytic performance.[8-10]

On the other hand, photocatalytic processes involving TiO_2 semiconductor particles under UV light illuminations have been shown to be potentially advantageous and useful in the treatment of organic pollutants.[18,19] However, they are limited to a considerable degree because of the high cost of their large-scale production, coupled with the low solar energy conversion efficiency and the high charge recombination rate of photogenerated electrons and holes.[19,20] In recent years, a large number of methods have been reported to improve the photocatalytic activity of TiO_2, including the doping of transition metal or non-metal ions,[21] the deposition of noble metals,[22] the surface sensitization of dyes[23] and the preparation of composite semiconductors.[24] Though the above modifications can partly improve the photocatalytic activity of TiO_2, there still exist some key problems unresolved, for example, complicated synthetic or modification procedures, doped materials suffer from a instability problem and difficulty in catalyst recycling. So from the point of view to remedy the environment, it is very urgent to develop TiO_2 based photocatalyst with simple synthetic procedures, high

activity, visible-response, high stability and easy recycling. Recently, it has been shown that TiO_2 hybridizing with a conducting polymer can increase the photocatalytic activity towards the decomposition of organic molecules when irradiated with visible light.[25]

Polyaniline (PANI) is one of the most frequently investigated conducting polymers for many reasons: it is environmentally stable, inexpensive, and its electrical conductivity can be easily tuned via special proton doping mechanism.[26] It is a conjugated polymer that can serve as an insulator, semiconductor, or conductor, depending on the degree of protonation and the preparation condition. Therefore, conjugated polymers with wide band gap inorganic semiconductors are receiving attention for optical, electronic, photocatalytic and photoelectric conversion applications.[27-29] Since conducting PANI behaves as a p-type semiconductor with a band gap absorption edge that can extend into the range of visible light and exhibits good environmental stability, the combination of TiO_2 and PANI should overcome the drawbacks of the former. Recently, the combination of PANI and TiO_2 to improve their performance of UV light,[29] sunlight[30] and visible light activity[25] has been reported. It shows PANI plays the role of photosensitizer and TiO_2 sensitized by PANI has enhanced photocatalytic activity. Furthermore, the doping type[31] and doping concentration[32] can play a significant role in determining the structural properties of PANI/TiO_2. Recently, Salem *etc.* have demonstrated the UV photocatalytic activity of PANI/TiO_2 formed in the presence of different acids follows the order: H_2SO_4>H_3PO_4>HCl>HNO_3 and decreases with the increase of HCl concentration,[29] which is different from our previous results that photocatalytic activity of PANI-TiO_2-HA prepared at pH 0.5 shows higher photocatalytic activity than that prepared at pH 1.5.[33] So even the effect of acid dopant in the preparation on the photocatalytic activity of PANI/TiO_2 under UV light irradiation has been investigated approximately, it may demonstrate different trend on the PANI-TiO_2-HA prepared in the presence of different acid at low temperature. And the reported work mainly focus on hybridizing PANI on the prepared or commercial TiO_2. The prepared or commercial TiO_2 usually involve in high-temperature thermal treatment to transform the amorphous TiO_2 into crystalline phase, which will lead to the TiO_2 nanoparticles aggregation, as well as the tendency of crystallites growth. Recently, some reports have demonstrated the fabrication of crystalline TiO_2 on halloysite minerals under mild conditons.[34,35] For example, a one-step solvothermal treatment at 180 °C is applied to prepare anatase/halloysite mineral composites, which demonstrate higher UV and visible light photocatalytic activity in decomposing NO_x gas. In our previous studies,[33,36] we have synthesized crystalline TiO_2-halloysite and PANI-crystalline TiO_2-halloysite composite nanotubes with HNO_3 as acid dopant and $FeCl_3$ as oxidant for PANI at low temperature and photocatalysis test results reveal the photocatalytic activity will be affected by the pH value and the volume ratio of ANI to TTIP. The highest photocatalytic activity is achieved with the composite photocatalysts prepared at pH 0.5 and 1% volume ratio of ANI and TTIP owing to the sensitizing effect of polyaniline and the effective charge transfer from the photoexcited PANI sensitizer to TiO_2.

In the present work, heterogeneous PANI-crystalline TiO_2-HA nanotubes are one-pot synthesized in the presence of various acids at low temperature by the similar procedure as that reported in reference 33. By simply adjusting the acidity of reaction system, PANI-crystalline TiO_2-HA composite nanotubes with different TiO_2 crystal phase and PAN redox state are obtained, where high temperature calcination is not required. Thus intact halloysite structure can be guaranteed and the growth of TiO_2 crystallites can be avoided. The effect of acid dopant in the preparation on the photocatalytic activities of PANI-TiO_2-HA heteroarchitectures under visible light irradiation are investigated systematically. Furthermore, the photocatalytic activity can be simply tuned by the type and concentration of acid dopant in the redoping process.

2. Experimental

2.1. Materials

The halloysite (HA) minerals were purchased from Imerys Tableware Asia Limited. Titanium isopropoxide (TTIP) was purchased from Nanjing Daoning Chemical Co., Ltd. Isopropyl alcohol, aniline (ANI) and ammonium persulfate ($(NH_4)_2S_2O_8$) were purchased from Sinopharm Chemical Reagent Co., Ltd. All reagents were analytical grade and used without further purification.

2.2. One-pot synthesis of heterogeneous PANI-TiO_2-HA nanotubes in the presence of different acid.

Titanium isopropoxide (TTIP) was used as precursor. To obtain the heterogeneous PANI-TiO_2-HA nanotubes without forming TiO_2 in the continuous media, the TTIP concentration was controlled at 0.01-0.05 M. In the preparation of heterogeneous PANI-TiO_2-HA nanotubes, TTIP, isopropyl alcohol and halloysite mineral's concentrations of different acidity system were fixed and the acidity of the system was adjusted by altering the feed amount of 2 M acid. The molar ratio of $(NH_4)_2S_2O_8$ to ANI was maintained at 1:1. The reaction temperature was controlled at 65 °C.[33,36] A typical procedure with HCl as pH tuning agent and acid dopant was as follows: TTIP (2 mL), isopropyl alcohol (30 mL), and hydrochloric acid (2 M, 79 mL) were mixed under stirring at room temperature for 1 h to form a concentrated transparent sol. By adding distilled water to the sol until a final volume of 500 mL, the final sol of pH 0.5 was obtained. Halloysite (HA, 1 g), aniline (ANI, 0.02 mL) and $(NH_4)_2S_2O_8$ (0.0499 g) were added to the above sol (500 mL) under stirring for 2 h. The dispersion was then heated at 65 °C for 24 h under stirring to form PANI-anatase/rutile-HA heteroarchitecture, which was denoted as P-TH/0.5/1%-HCl. The acidity of the sol and PANI content were adjusted by altering the feed amount of 2M acid and ANI, respectively. In this way, PANI-TiO_2-HA composite nanotubes with 1% volume ratio of ANI to TTIP in the presence of HNO_3, H_2SO_4 and H_3PO_4 were prepared; these were labeled as P-TH/0.5/1%-HNO_3, P-TH/0.5/1%-H_2SO_4 and P-TH/0.5/1%-H_3PO_4, respectively. Similarly, PANI-TiO_2-HA composite nanotubes prepared at the initial pH of the TiO_2 sol of 1.5 with 1% volume ratio of ANI to TTIP in the presence of HNO_3, HCl, H_2SO_4 and H_3PO_4.were denoted as P-TH/1.5/1%-HNO_3, P-TH/1.5/1%-HCl, P-TH/1.5/1%-H_2SO_4 and P-TH/1.5/1%-H_3PO_4, respectively. To confirm the sensitization effect of PANI on the photocatalytic activities of the composite nanotubes, the TiO_2-HA composite nanotubes (TH/1.5-HCl, TH/0.5-HCl) in the presence of HCl were prepared with the same procedure as that of the heterogeneous PANI-crystalline TiO_2-HA nanotubes except that ANI and $(NH_4)_2S_2O_8$ were not added. The PANI-TiO_2-HA heteroarchitectures (P-TH/X/Y-Z) were separated by centrifugation, washed with water several cycles to neutral and

transferred to oven to dry at 65 °C.

2.3. Characterization

Heterogeneous PANI-TiO_2-HA nanotubes (P-TH/X/Y-Z) were dispersed in ethanol and spread onto carbon-coated copper grids for TEM (JSM-2100) equipped with an energy dispersive X-ray spectrum (EDX, Inca Energy-200) at an accelerating voltage of 200 kV. Wide-angle X-ray powder scattering (XRD, Rigaku D/max-3B) with Cu Kα radiation was used to characterize the crystalline phases in the 2θ range 5-90° at a scan rate of 10°/min. FT-IR measurements were performed on a Thermo Nicolet 8700 instrument. Potassium bromide pellets containing 0.5% of the samples were used in FT-IR experiments and 64 scans were accumulated for each spectrum in absorbance at a spectral resolution of 2 cm^{-1}. The spectrum of dry KBr was taken for background subtraction. UV-vis diffuse reflectance spectra were measured at room temperature in air on a Shimadzu UV-2401PC photometer over the range from 200 to 800 nm. X-ray photoelectron spectroscopy (XPS) measurements were performed with an ESCALab220i-XL electron spectrometer from VG Scientific using 300W Al Kα radiation. The base pressure was about 3×10^{-9} mbar. The binding energies were referenced to the C1s line at 284.6 eV from adventitious carbon. Electrical conductivity measurements were performed with Agilent 4294 impedance analyzers at the room temperature. The testing frequency was 40Hz-110MHz. The samples were pressed into a 12.8 mm diameter disk for the measurement.

2.4. Measurement of photocatalytic activity

The reactions of the photocatalytic degradation of dyes in solution were carried out in a quartz batch photoreactor containing 50 mL 10 mg/L rhodamine B (RB) solution and 25 mg of the heterogeneous PANI-TiO_2-HA nanotubes (P-TH/X/Y-Z). The suspensions were magnetically stirred in the dark for 24 h to attain adsorption-desorption equilibrium between RB and P-TH/X/Y-Z. Subsequently, the photocatalytic degradation experiments of RB over P-TH/X/Y-Z under visible light irradiation were performed using XPA-7 photochemical system (Xujiang Electromechanical Plant, Nanjing, China). A 800 W Xe lamp ($290< \lambda < 800$ nm) with optical filter to eliminate the UV emission below 400 nm was used as visible light resource[33,36] and the emission intensity on the suspensions surface was 24 mW/cm^2. During the photocatalytic experiments, the quartz batch photoreactor without degassed was sealed in order to avoid the decrease of the volume of the suspension and kept under constant stirring without purged with inert gas and air (O_2). Adequate aliquots (6 mL) of the sample were withdrawn in the air after periodic intervals of irradiation, which were centrifuged at 4 000 rpm for 10 min, and then filtered through a microporous filter (pore size 0.45 μm) to remove the residual catalyst particulates for analysis. The concentration of filtrates was determined by recording the maximum absorbance of RB at 553 nm with UV1800 photometer over the range from 200 to 800 nm.

3. Results and discussion

3.1. Characterization of the heterogeneous PANI-TiO_2-HA nanotubes

A commercial halloysite mineral is selected as an example parent support for preparing the heterogeneous PANI-crystalline TiO_2-HA nanotube. The structure and morphology of the halloysite mineral are characterized with SEM and TEM. As shown in Fig. S1a, the halloysite predominately consists of cylindrical tubes 40-60 nm in diameter and 1-2 μm in length. TEM image reveals the empty lumen structure of halloysite mineral and the inner diameter is 20-30 nm (Fig. S1b in ESI†). Periodicity in the individual layer packing is determined with XRD and is found to be 0.73±0.02 nm, which corresponds to dehydrated halloysite (Fig. S2 in ESI†). XPS and EDX demonstrate that elemental composition of the halloysite is as follows (atomic %): Al, 17.6; Si, 17.5; O, 64.9 (Fig. S3, Fig. S4 in ESI†). Elements like Ca, Fe, Cu and Na are not detected. The BET surface area of the halloysite minerals is 38.6 m^2/g.[36] The above data prove that the support is a halloysite rich mineral. It is well known that pH value controlled to a relatively low value (pH<2) is crucial to facilitate the formation of crystalline TiO_2.[37] Under such condition, the growing crystalline TiO_2 species such as $[Ti(OH)_x(OH_2)_{6-x}]^{(4-x)+}$ are positively charged,[37] because the pH value is lower than the isoelectric point of TiO_2 (pH 5-7). In our previous paper, we have proved that when the pH is lower than 2, the outer surface of the tubular halloysite minerals is negatively charged and can induce the inorganic TiO_2 nanocrystals and PANI to grow onto the tubular halloysite minerals *in situ* in the presence of HNO_3 with $FeCl_3$ as oxidant at low temperature.[33] In this study, we synthesize heterogeneous PANI-crystalline TiO_2-HA nanotubes at low temperature by the similar procedure as that of preparing the heterogeneous PANI-crystalline TiO_2-HA

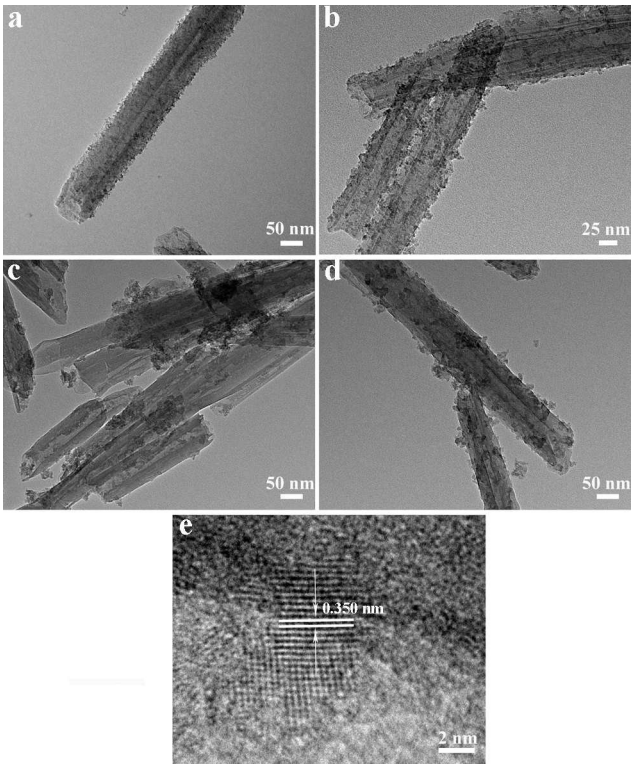

Fig. 1 TEM images of the heterogeneous PANI-TiO_2-HA nanotubes prepared at pH 1.5 of the starting sols by one-pot with 1% volume ratio of ANI to TTIP (P-TH/1.5/1%-Z): the pH of the starting sols is tuned by a) HNO_3, b) HCl, c) H_2SO_4 and d) H_3PO_4; e) HRTEM image of the sample as shown in (b), revealing the anatase phase structure.

nanotubes in the presence of HNO_3, HCl, H_2SO_4 and H_3PO_4 with $(NH_4)_2S_2O_8$ as ANI's oxidant. By simply adjusting the acidity of reaction system, TiO_2 crystalline phase and PANI redox state can be tuned. And by tuning the acid dopant in the preparation, the visible light photocatalytic activity of polyaniline-crystalline TiO_2-halloysite composite nanotubes can be tuned. In the previous study,[33] it shows the optimum volume ratio of ANI to TTIP is 1% for the enhanced photocatalytic activity of PANI-TiO_2-HA, so in the present work, the photocatalytic activity of PANI-TiO_2-HA prepared in the presence of different acid and with 1% volume ratio of ANI to TTIP (P-TH/X/1%-Z) is investigated mainly.

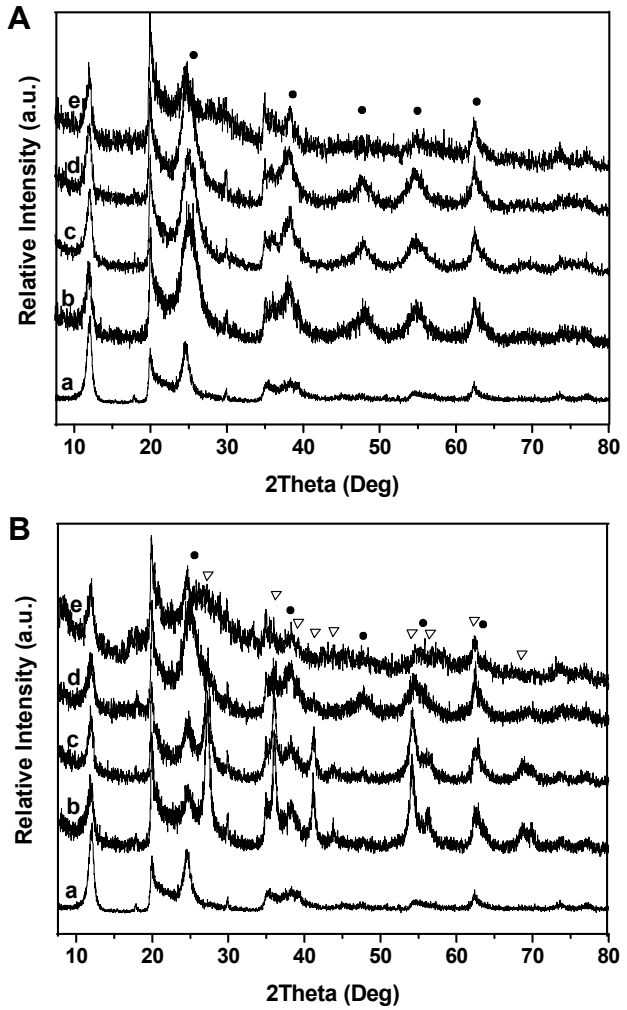

Fig. 2 XRD spectra of heterogeneous PANI-TiO_2-HA nanotubes prepared by one-pot with 1% volume ratio of ANI to TTIP at pH 1.5 (A) and 0.5 (B) of the starting sols: a) HA; the pH of the starting sols is tuned by b) HNO_3, c) HCl, d) H_2SO_4 and e) H_3PO_4, respectively. ▽: rutile (JCPDS No. 21-1276); ●: anatase (JCPDS No. 21-1272).

At an initial pH value of 1.5, heterogeneous PANI-TiO_2-HA nanotubes with coarse surfaces are obtained (Fig. 1) and noted as P-TH/1.5/1%-Z. Compared with the parent halloysite support, 3-10 nm grains are homogeneously deposited on the surfaces of tubular halloysite minerals without visible aggregation. The hollow lumen of the P-TH/1.5/1%-Z heteroarchitecture is discerned clearly (Fig. 1). The anatase phase is verified by high resolution TEM (HRTEM) (Fig. 1e) and XRD (line b-e in Fig. 2A). The TiO_2 in rutile phase gradually appears as increasing the acidity of the starting sol. As an example, at pH value of the TiO_2 sol of 0.5, the representative heterogeneous nanotubes are obtained with anatase/rutile phases coexisting (Fig. 2B, Fig. 3), which are cited as P-TH/0.5/1%-Z. Fig. 3 shows that some nanosized needles or larger nanoparticles are grown and protruded from the coarse anatase surface at pH 0.5 for P-TH/0.5/1%-HNO_3 and P-TH/0.5/1%-HCl. And the heterogeneous P-TH/0.5/1%-HNO_3 and P-TH/0.5/1%-HCl composite nanotubes have two distinct regions in morphology, the nanoneedles (or larger nanoparticles) and the nanograins, labeled as A and B in Fig. 3b, respectively. HRTEM (Fig. 3e,f) results reveal that the needles of region A are in rutile phase with a (110) lattice spacing of 0.324 nm, where nanograins in region B, which correspond to the coarse surface, are identified as anatase phase with a (101) lattice spacing of 0.350 nm (Fig. 3f). It has to mention that the morphology of PANI-TiO_2-HA composite nanotubes prepared at pH 0.5 in the presence of different acid dopant is different: nanoneedles and the nanograins coexist on the surface of HA for the PANI-TiO_2-HA with HNO_3 (P-TH/0.5/1%-HNO_3) and HCl (P-TH/0.5/1%-HCl) tuning the pH and as acid dopant, whereas 50-100 nm nanograins and irregular grains are observed on the surface of HA for the PANI-TiO_2-HA with H_2SO_4 (P-TH/0.5/1%-H_2SO_4) and H_3PO_4 (P-TH/0.5/1%-H_3PO_4) tuning the pH and as acid dopant, respectively. Furthermore, there are no PANI and TiO_2 in the bulk except the P-TH/0.5/1%-H_3PO_4 reaction system,

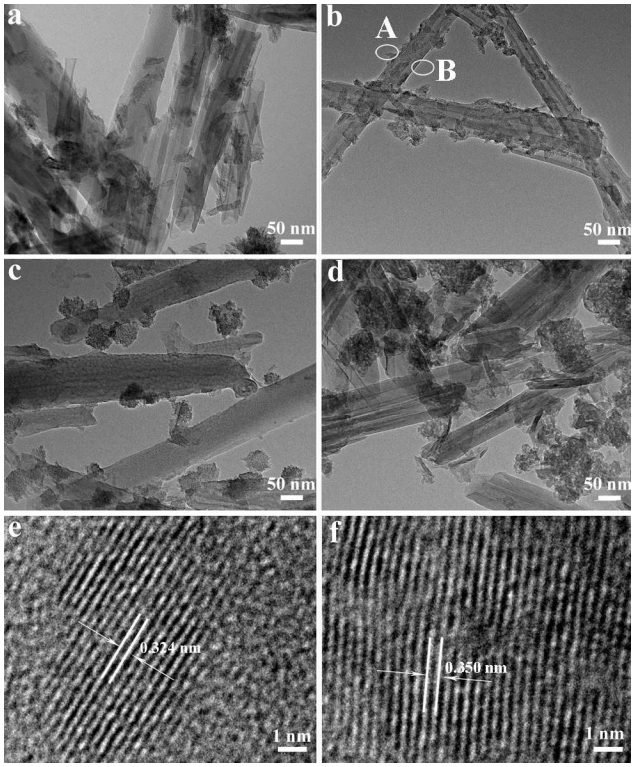

Fig. 3 TEM images of the heterogeneous PANI-TiO_2-HA nanotubes prepared at pH 0.5 of the starting sols by one-pot with 1% volume ratio of ANI to TTIP (P-TH/0.5/1%-Z): the pH of the starting sols is tuned by a) HNO_3, b) HCl, c) H_2SO_4 and d) H_3PO_4; e, f) HRTEM images of regions A and B, respectively, of the sample shown in b), revealing the anatase/rutile mixed phase structure.

indicating halloysite can induce TiO_2 nanocrystalline and PANI to grow on the halloysite mineral *in situ* simultaneously. Although the morphology of P-TH/0.5/1%-H_2SO_4 is different from those of P-TH/0.5/1%-HCl and P-TH/0.5/1%-HNO_3, HRTEM and XRD (line d in Fig. 2B) indicate the TiO_2 is anatase/rutile mixed phase structure.

The FT-IR spectra of heterogeneous PANI-TiO_2-HA nanotubes prepared at pH 1.5 (P-TH/1.5/1%-Z) and pH 0.5 (P-TH/0.5/1%-Z) with 1% volume ratio of ANI to TTIP are shown in Fig. S5A and Fig. S5B, respectively. For comparison, the spectra of parent halloysite (line a in Fig. S5 in ESI†) is also given. Unfortunately, the main characteristic peaks of PANI are not clear owing to the low volume ratio of ANI to TTIP (1%). In order to well characterize the PANI in PANI-TiO_2-HA, the spectra of PANI-TiO_2-HA with 100% volume ratio of ANI to TTIP prepared under the similar condition are shown in Fig. 4A and Fig. 4B, respectively. The main characteristic peaks of PANI in P-TH/X/100%-HCl prepared at pH 1.5 and pH 0.5 are assigned as follows: the band at 3412 (3414) cm^{-1} is attributed to N–H

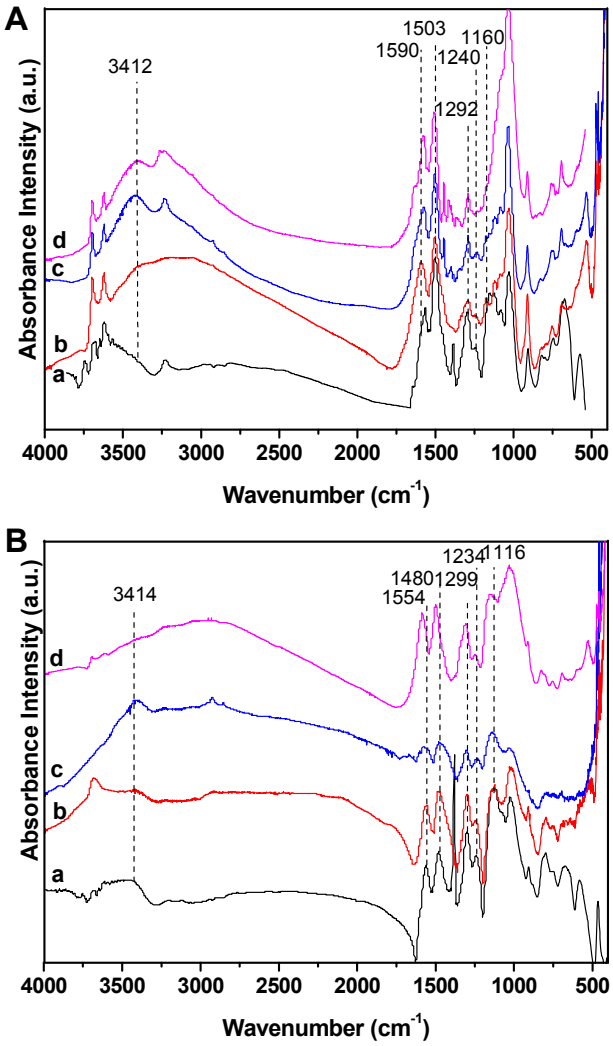

Fig. 4 FT-IR spectra of heterogeneous PANI-TiO_2-HA nanotubes prepared by one-pot with 100% volume ratio of ANI to TTIP at pH 1.5 (A) and 0.5 (B) of the starting sols: the pH of the starting sols is tuned by a) HNO_3, b) HCl, c) H_2SO_4 and d) H_3PO_4, respectively.

stretching mode;[38] the absorption peaks at 1590 (1554) and 1240 (1234) cm^{-1} correspond to the C=C stretching vibration and C–H stretching vibration of quinoid ring; the peaks at 1503 (1480) and 1292 (1299) cm^{-1} are related to the C=C stretching vibration and C–N stretching vibration of benzenoid ring; the band at 1160 (1116) cm^{-1} is due to the quinonoid unit of doped PANI.[26-32,33] The values outside bracket and in bracket, respectively are PANI characteristic peaks prepared at pH 1.5 and pH 0.5. The PANI peaks around 1292 (1299), 1503 (1480) and 1590 (1554) cm^{-1} denote there are two forms of PANI, pernigraniline and leucoemeraldine in the PANI-TiO_2-HA prepared at pH 1.5 and pH 0.5. As shown in Fig. 4a,c,d, the peaks related to the groups of PANI also appear in the FT-IR spectra of heterogeneous PANI-TiO_2-HA nanotubes with HNO_3, H_2SO_4 and H_3PO_4 tuning the pH in the preparation, indicating a successful growing of PANI. Comparing to the P-TH/X/100%-HCl, the corresponding peaks of PANI in the composite clay nanotubes with other acid dopant tuning the pH suffer some degree of deviation: those in the P-TH/X/100%-H_2SO_4 have a tiny difference, whereas those in the P-TH/X/100%-H_3PO_4 shift to lower (pH 1.5) and higher wavenumbers (pH 0.5); those in the P-TH/1.5/100%-HNO_3 shift to lower wavenumbers, suggesting that different interaction exists between TiO_2 nanoparticles and PANI.[26-32,33] Furthermore, by comparing PANI characteristic stretching bands in the range of 1600-1150 cm^{-1} for P-TH/1.5/100%-Z (Fig. 4A) and P-TH/0.5/100%-Z (Fig. 4B), the peaks of P-TH/0.5/100%-Z are shifted to a lower wavenumber and the ratio of quinoid unit to benzenoid is about one, indicating the PANI in P-TH/0.5/100%-Z is emeralding (EM),[26] whereas in P-TH/1.5/100%-Z, a high fraction of pernigraniline (PNA) form is **present**. Furthermore, as the band at 1160 (1116) cm^{-1} is ascribed to the quinonoid unit of doped PANI, so by comparing the peak intensity at 1160 (1116) cm^{-1} and 1590 (1554), the doped degree of quinonoid unit can be calculated. From Fig. 4, the peak intensity ratio of 1116/1554 for PANI-TiO_2-HA prepared at pH 0.5 is higher than that of 1160/1590 for PANI-TiO_2-HA prepared at pH 1.5, indicating higher doped degree and electrical conductivity for P-TH/0.5/100%-Z.

To illustrate the controllable PANI content by tuning the volume ratio of ANI to TTIP, the FT-IR of heterogeneous PANI-TiO_2-HA nanotubes prepared with different volume ratio of ANI to TTIP in the presence of HCl at pH 1.5 and 0.5 of the starting

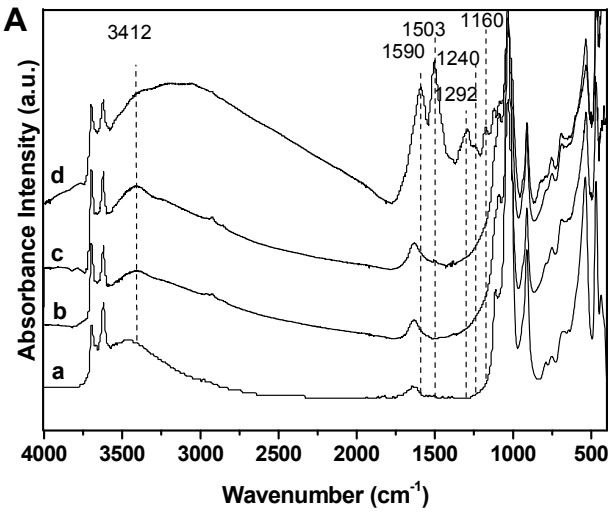

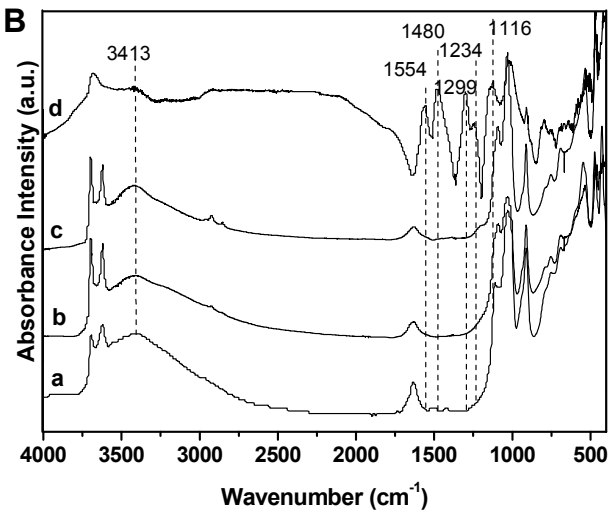

Fig. 5 FT-IR spectra of heterogeneous PANI-TiO_2-HA nanotubes prepared by one-pot with different volume ratio of ANI to TTIP at pH 1.5 (A) and 0.5 (B) of the starting sols: a) 0%, b) 1%, c) 5% and d) 100%. The pH of the starting sols is tuned by 2M HCl solution.

sols are given in Fig. 5. It can also be observed that with the increase of volume ratio of ANI to TTIP, the intensity of the PANI characteristic peaks also increases, implying PANI content can be simply tuned by the volume ratio of ANI to TTIP. P-TH/1.5/Y-Z and P-TH/0.5/Y-Z also show the characteristic bands of halloysite, such as the stretching vibration of the inner-surface hydroxyl groups of Al_2OH at 3694 and 3620 cm^{-1}, the deformation vibration of the above hydroxyl groups at 912 cm^{-1}, and the deformations vibration of Al-O-Si and Si-O-Si at 536 and 468 cm^{-1}.[12,33,36] Interlayer or adsorbed water is indicated by the stretching vibration at 3450 cm^{-1} and the corresponding deformation vibration at 1630 cm^{-1}. The reflections of the FT-IR spectra indicate that the structure of halloysite minerals remain unaffected by the PANI-TiO_2 treatment.

The protonated state in the heterogeneous PANI-TiO_2-HA nanotubes is further studied by UV-vis absorption spectra. UV-vis spectra of P-TH/1.5/1%-Z and P-TH/0.5/1%-Z are shown in Fig. 6A and Fig. 6B, respectively. For comparison, the spectra of parent halloysite minerals (line a in Fig. 6), TiO_2-HA nanotubes prepared at pH 1.5 (TH/1.5-HCl), TiO_2-HA nanotubes prepared at pH 0.5 (TH/0.5-HCl) with HCl tuning the pH and P25 are also given. It shows all the P25, TiO_2-HA nanotubes and PANI-TiO_2-HA absorb light below 400 nm. The main difference of PANI-TiO_2-HA (P-TH/X/1%-Z) from P25 and TiO_2-HA nanotubes is it absorbs light giving rise to a peak at 450 nm and a broad peak in the range of 470-800 nm, respectively characteristic of the π-π* transition of benzenod ring and polaron-π* transitions of quinoid ring,[26,33] indicating the presence of the PANI on the surface of HA and two forms of PANI, pernigraniline and leucoemeraldine in the P-TH/X/Y-Z. Furthermore, the absorption intensity in the visible light region presents such a trend: P-TH/X/1%-HCl>P-TH/X/1%-H_2SO_4>P-TH/X/1%-HNO_3>P-TH/X/1%-H_3PO_4. And comparing to the peak start of the broad peak in the range 470-800 nm of PANI-TiO_2-HA prepared at pH 1.5 (Fig. 6A, marked with dash line), the peak start of PANI-TiO_2-HA prepared at pH 0.5 are red shifted (Fig. 6B, marked with dash line), signifying PANI form prepared at pH 0.5 is more closer to the EM form.[39] In comparison to halloysite mineral,[33,36] the absorption attributed to crystalline TiO_2 around 400 nm is present, which further confirms that the crystalline TiO_2 is successfully grown on the surface of halloysite minerals for the P-TH/1.5/1%-Z and P-TH/0.5/1%-Z samples. For P-TH/0.5/1%-Z, the absorption edge (Fig. 6B) shows a greater red shift than that of P-TH/1.5/1%-Z due to the presence of rutile phase (band gap energy: 3.0 eV). The above results imply that PANI/TiO_2 has been successfully grown on the surface of halloysite mineral and the PANI-TiO_2-HA with HCl tuning the pH and as acid dopant in the preparation has the strongest absorption in the visible light region.

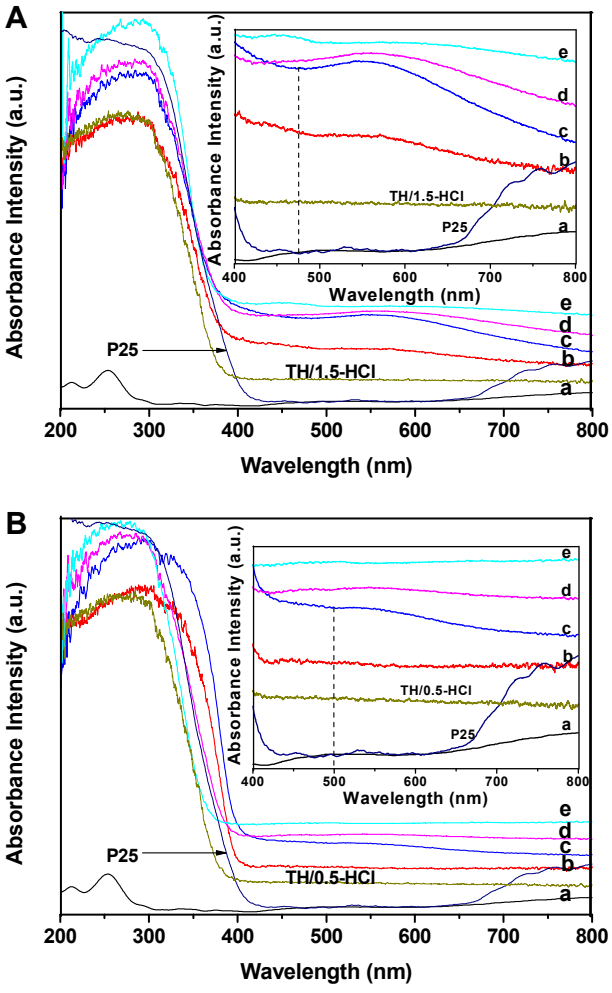

Fig. 6 UV-vis spectra of heterogeneous PANI-TiO_2-HA nanotubes prepared by one-pot with 1% volume ratio of ANI to TTIP at pH 1.5 (A) and 0.5 (B) of the starting sols: a) HA, the acidity is tuned by b) HNO_3, c) HCl, d) H_2SO_4 and e) H_3PO_4, respectively.

The composition of P-TH/X/1%-Z is further confirmed by EDX spectra analysis and the result is shown in Table S1. The electrical conductivity data of P-TH/X/1%-Z shows the conductivity increases with the decrease of pH at the same acid tuning the pH and as acid dopant in the preparation. Moreover, at the same pH, the heterogeneous PANI-TiO_2-HA composite nanotube with HCl tuning the pH value in the preparation demonstrate the highest conductivity, followed by P-TH/X/1%-H_2SO_4 and P-TH/X/1%-HNO_3, and P-TH/X/1%-H_3PO_4 has the minimum conductivity, which are consistent with the results of

UV-vis. The above results indicate by simply tuning the acid dopant in the preparation, the conductivity of PANI-TiO_2-HA composite nanotubes can be tuned.

3.2. Photocatalytic activities of the heterogeneous PANI-TiO_2-HA nanotubes (P-TH/X/Y-Z) under visible light irradiation

To demonstrate the influence of acid dopant in the preparation on the photocatalytic activity of the PANI-TiO_2-HA heteroarchitectures for the degradation of organic pollutants, the photocatalytic degradation of rhodamine B (RB) is carried out under visible light irradiation. Furthermore, 25 mg of P25, 10 ppm RB aqueous solution are used as photocatalytic references to illustrate the photocatalytic activity of the PANI-TiO_2-HA heteroarchitectures more clearly. Photodegradation yield is defined as:

$$\text{Photodegradation yield} = \frac{C_0 - C_a - C_b}{C_0}$$

where C_0 is the concentration of dye after 24 h adsorption-desorption equilibrium in the dark, C_a is the concentration after photodegradation of dye and C_b is the decreased concentration because of the direct photolysis. RB shows a maximum absorption at about 553 nm. Total concentrations of the dyes are determined by the maximum absorption measurement.

The adsorption capacity of the PANI-TiO_2-HA composite nanotubes prepared by one-pot in the presence of different acid (P-TH/X/1%-Z), P25, TH/0.5-HCl and TH/1.5-HCl are firstly investigated. From Table S2, it can be seen that the introduction of PANI into the composite clay nanotube improves their adsorption capacities in the dark. The adsorption capacity of P-TH/X/1%-Z composites nanotube with different acid tuning the pH in the preparation is different. The maximum adsorption capacity of the P-TH/0.5/1%-Z is observed when H_3PO_4 is used to tune the pH in the preparation. The change in the adsorption capacity of P-TH/X/Y composites with acid dopant tuning the pH in the preparation may be derived from the differences in the size and nature of the dopant anion in PANI.

Fig. 7 shows the photodegradation curves of RB under visible light irradiation on the P-TH/X/1%-Z, P25 and the self-degradation of RB. It is found that the self-degradation of RB is not obvious, indicating the stabilization of RB under visible light irradiation. However, in the presence of P-TH/X/1%-Z, the degradation of RB are obvious, especially in the presence of P-TH/X/1%-Z with HCl tuning the pH in the preparation and low pH value. PANI-TiO_2-HA composite nanotubes prepared by one-pot at pH 0.5 with HCl tuning the pH in the preparation (P-TH/0.5/1%-HCl) have the highest photocatalytic activity among all the test samples, which may be attributed to the mixed anatase/rutile phase structure of P-TH/0.5/1%-HCl and the EM form of PANI.[19,33,36] In comparison, only 76.5% of RB molecules for TH/0.5-HCl (prepared at pH 0.5 with HCl tuning the pH in the preparation and without PANI) are decomposed in 6 h, indicating PANI can enhance the photocatalytic degradation of RB. Whereas after exposed under visible light irradiation for 6 h, the degradation efficiency of RB for P-TH/1.5/1%-HCl is higher than that of TH/1.5-HCl, whereas in our previous report,[33] the photocatalytic activity of P-TH/1.5/1% with HNO_3 tuning the pH is lower than that of TH/1.5 with HNO_3 tuning the pH, implying photocatalytic efficiency will be affected by the acid dopant in the preparation. The photocatalytic degradation efficiency of

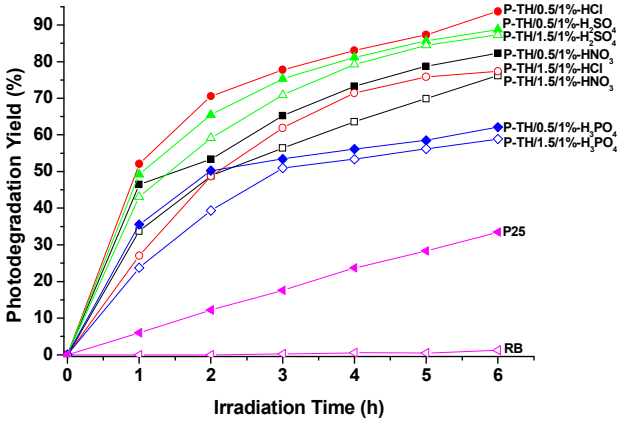

Fig. 7 Comparison of photodegradation yield of PANI-TiO_2-HA composite nanotubes prepared by one-pot in the presence of different acid (P-TH/X/1%-Z) for degradation of RB under visible light irradiation.

degradation efficiency will be affected by the pH value. The photocatalytic activity of the PANI-TiO_2-HA composite nanotubes follows the order: P-TH/0.5/1%-HCl>P-TH/0.5/1%-H_2SO_4>P-TH/1.5/1%-H_2SO_4>P-TH/0.5/1%-HNO_3>P-TH/1.5/1%-HCl>TH/0.5-HCl>P-TH/1.5/1%-HNO_3>TH/1.5-HCl>P-TH/0.5/1%-H_3PO_4>P-TH/1.5/1%-H_3PO_4>P25. Obviously, it can be observed the acid dopant in the preparation process will affect the photocatalytic efficiency of P-TH/X/1%-Z. At the same pH value, the photocatalytic degradation efficiency follows the sequence: P-TH/X/1%-HCl>P-TH/X/1%-H_2SO_4>P-TH/X/1%-HNO_3>P-TH/X/1%-H_3PO_4. The reason for the phenomenon is explained below. From Table S1and Fig. 6 (inset), it exhibits the electrical conductivity and absorption intensity in the visible light region presents such a trend: P-TH/X/1%-HCl>P-TH/X/1%-H_2SO_4>P-TH/X/1%-HNO_3>P-TH/X/1%-H_3PO_4. When the absorption intensity in the visible light region for P-TH/X/1%-Z is high, the catalyst can absorb more visible light and generate more electron-hole pairs. Furthermore, as it also has higher electrical conductivity and matched well in energy level of TiO_2 and PANI, the electrons generated from PANI under visible light irradiation can be effectively transferred into the CB of TiO_2. Therefore, the photocatalytic activity of P-TH/X/1%-HCl for RB is enhanced due to efficient visible light absorption and charge separation.

Meanwhile, with the same acid tuning the pH in the preparation process, P-TH/X/1%-Z composite nanotube prepared at lower pH demonstrates higher photocatalytic degradation efficiency. Interpretation of such negative effect of the pH on the current photocatalytic degradation is a very difficult task because of the possible contribution of both the TiO_2 and PANI in that effect. In our previous work,[33] we have proved by redoping P-TH/1.5 experiment that the PANI redox state plays the main contribution to the enhanced visible light catalytic degradation efficiency of P-TH/0.5/Y. So we do not discuss the reason in details here.

Furthermore, photocatalytic activities of the PANI-TiO_2-HA heteroarchitectures with HCl tuning the pH and different volume ratio of ANI to TTIP in the preparation (P-TH/X/Y-HCl) for the

degradation of RB under visible light irradiation are also investigated. From Fig. S6, it is obvious the visible light photocatalytic activity of P-TH/0.5/Y-HCl (prepared at pH 0.5) is higher than that of P-TH/1.5/Y-HCl (prepared at pH 1.5) on the degradation of RB at the same volume ratio of ANI to TTIP, which is consistent with the photocatalytic degradation result of the P-TH/X/1%-Z (Fig. 7). At the same pH value, the photocatalytic degradation efficiency decreases with the increase of the volume ratio of ANI to TTIP from 1% to 100% and an optimum of the sensitized effect is found when the volume ratio of ANI to TTIP is 1%. We ascribe to the synergetic effect of the electron-hole pairs production and separation between PANI and TiO_2, which is accordant with the previous result of PANI-TiO_2-HA prepared with HNO_3 tuning the pH value and $FeCl_3$ as ANI's oxidant in the preparation.[33]

From the photocatalytic results we have gathered, it is consistent that the acid type used for tuning the pH value and as acid dopant, pH value and the volume ratio of ANI and TTIP in the preparation will affect the photocatalytic efficiency and the highest photocatalytic activity is achieved on the PANI-TiO_2-HA prepared at pH 0.5, with HCl tuning the pH and 1% volume ratio of ANI to TTIP in the preparation (P-TH/0.5/1%-HCl). Furthermore, it is worth mentioning the photocatalytic activity of PANI-TiO_2-HA can be tuned by tuning the concentration and type of acid dopant in the redoping process. To illustrate this situation, P-TH/0.5/1%-HCl and P-TH/1.5/1%-HCl are redoped with acid dopant of different concentrations and varieties. Fig. 8 shows the photodegradation curves of RB under visible light irradiation on the P-TH/X/1%-HCl composite nanotubes after redoped with different concentrations of HCl. The redoped sample is cited as P-TH/X/1%-HCl-G. G is the concentration of acid dopant. For example, when the HA-TiO_2-PANI prepared at pH 0.5 with 1% volume ratio of ANI to TTIP and HCl as dopant acid in the preparation (P-TH/0.5/1%-HCl) is redoped with 0.5 M HCl, it is denoted as P-TH/0.5/1%-HCl-0.5 M HCl, whereas when it is redoped with 0.17 M H_3PO_4, it is denoted as P-TH/0.5/1%-HCl-0.17 M H_3PO_4. It shows the optimal redoping concentration is 0.5 M. After redoped with HCl at the same concentration, the photocatalytic activity of P-TH/0.5/1%-HCl is still higher than that of P-TH/1.5/1%-HCl, we attribute this to the mixed structure of TiO_2 in P-TH/0.5/1%-HCl. For comparison, the photocatalytic activity of the PANI prepared at the same acidity is also given. Although the photocatalytic activity of PANI is lower than that of P-TH/0.5/1%-HCl-G, it still demonstrates that the PANI prepared at 0.5 M HCl (PANI/0.5 M HCl) has the highest photocatalytic activity, which is accordant with the photocatalytic activity trend of P-TH/X/1%-HCl-G. In order to find the relationship between electrical conductivity and photocatalytic activity, the electrical conductivity of the pure PANI prepared at varied acidity is given (Table S1). It can be seen the electrical conductivity increases with the acidity in the range of 0.0316 M (pH 1.5)-2 M. Combined with the photocatalytic activity data, it can be concluded that the enhanced photocatalytic activity can be achieved at an optimum electrical conductivity of PANI. What is more, by redoping the P-TH/X/1%-HCl with 0.25 M H_2SO_4 and 0.17 M H_3PO_4, comparable to the acidity of 0.5 M HCl, the photocatalytic activity of P-TH/X/1%-HCl-G decreases, although the concentration of acid dopant can be regarded as similar (Fig. S7 in ESI†), meaning by tuning the type of acid in the redoping process, the photocatalytic acidity can be tuned.

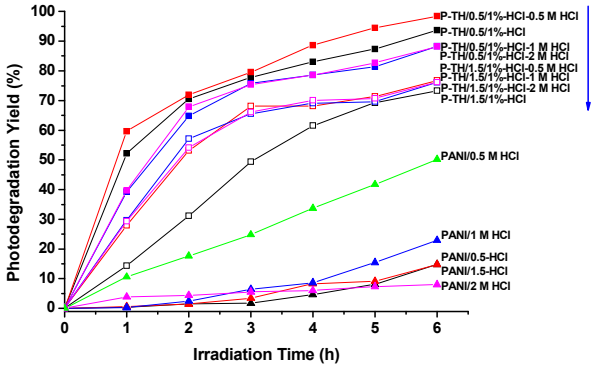

Fig. 8 Comparison of photodegradation yield of P-TH/X/1%-HCl after being doped with HCl solution for degradation of RB under visible light irradiation.

3.3. Mechanism of the different visible photocatalytic activity of the heterogeneous PANI-TiO_2-HA nanotubes by tuning the acid dopant in the preparation.

On the basis of the results of photocatalytic tests, it shows the heterogeneous PANI-TiO_2-HA composite nanotubes with different acid tuning the pH and as acid dopant in the preparation have different visible light photocatalytic activity: P-TH/X/1%-HCl demonstrates the highest photocatalytic activity, followed by P-TH/X/1%-H_2SO_4 and P-TH/X/1%-HNO_3, and P-TH/X/1%-H_3PO_4 has the minimum photocatalytic activity at the same pH value. And UV-vis and electrical conductivity test for the light absorption in the visible light region and electrical conductivity also present similar trend. It is reported that TiO_2 and PANI are matched well in energy level: the conduction band (CB) position of TiO_2 is lower than the LUMO of PANI, so the former can act as a sink for the photogenerated electrons in the hybrid photocatalysts; the valence band (VB) position of TiO_2 is lower than the HOMO of PANI, so the later can act as an acceptor for the photogenerated holes in the hybrid photocatalysts.[28-30,33] Therefore, when the PANI-TiO_2-HA composite nanotube with enhanced visible light absorption and electrical conductivity is illuminated under visible light, more visible light is absorbed and more electron-hole pairs is generated, the electrons generated from PANI can be effectively transferred into the CB of TiO_2, while some positive carbon radicals in PANI are formed, as well as in a dye-sensitized TiO_2 system. These positive carbon radicals may be reduced by an electron from organic pollutants or water, or react with oxygen to generated active species (hydrogen radical, singlet/triplet oxygen) which are capable of degrading organic pollutants. So herein, effective visible light absorption, reducing the recombination probability and making charge separation more efficient lead to a higher photocatalytic activity with the heterogeneous PANI-TiO_2-HA nanotubes prepared with HCl tuning the pH in the preparation.

4. Conclusions

We have proposed a facile method to synthesize heterogeneous

PANI-crystalline TiO_2-HA nanotubes with enhanced visible light photocatalytic activity by tuning the acid dopant in the preparation. By simple adjustment of the acidity of the TiO_2 sol at 65 °C, PANI-crystalline TiO_2-HA composite nanotubes composed of anatase, a mixed-phase TiO_2 and different PANI redox state can be produced. The degradation of RB in an aqueous solution under visible light irradiation is carried out to evaluate the photocatalytic activity of the resulting composite photocatalysts. It shows photocatalytic activity will be affected by the type of acid dopant, pH value and the volume ratio of ANI to TTIP in the preparation and the highest photocatalytic activity is achieved with the composite photocatalysts prepared with HCl tuning the acidity at pH 0.5 and 1% volume ratio of ANI and TTIP (P-TH/0.5/1%-HCl). This can be attributed to the effective visible light absorption and charge separation. Furthermore, redoping P-TH/0.5/1%-HCl with different concentration of HCl and acid dopant (H_2SO_4 and H_3PO_4) demonstrates redoping with 0.5 M HCl has the highest photocatalytic activity and its photocatalytic activity decreases when redoped with H_2SO_4 and H_3PO_4, indicating by tuning the concentration and type of acid dopant in the redoping process, the photocatalytic acidity can be tuned.

Acknowledgment

The authors gratefully acknowledge the financial support of the National Natural Science Foundation of China (Nos. 51563023, 51003091), the Applied Basic Foundation of Yunnan Province (No. 2013FB002), the Education Research Foundation of Yunnan Province (Nos. 2013Y361, 2010Y240), the Research Foundation of Yunnan University (No. 2009B06Q) and Backbone Teacher Training Program of Yunnan University (No. XT412003).

Notes and references

Department of Applied Chemistry, Key Laboratory of Medicinal Chemistry for Natural Resource, Ministry of Education, School of Chemical Science and Technology, Yunnan University, Kunming 650091, China. Fax: +86 871 6503 1567; Tel: +86 871 6503 1567; E-mail: licp830@iccas.ac.cn

† Electronic Supplementary Information (ESI) available: SEM and TEM images, XRD, XPS and EDX of the halloysite (HA) minerals (Fig. S1-Fig. S4), FT-IR spectra of heterogeneous P-TH/X/1%-Z (Fig. S5), mass ratio of PANI to TiO_2 and conductivity of P-TH/X/Y-Z (Table S1), the adsorption ratio of P-TH/X/1%-Z for RB (Table S2), photodegradation yield of P-TH/X/Y-HCl (Fig. S6) and P-TH/X/1%-HCl after being doped with 0.5 M HCl, 0.25 M H_2SO_4 and 0.17 M H_3PO_4 solution (Fig. S7). See DOI: 10.1039/b000000x

1 T. S. Wu, K. X. Wang, G. D. Li, S. Y. Sun, J. Sun and J. S. Chen, *ACS Appl. Mater. Interfaces*, 2010, **2**, 544.
2 G. K. Zhang, X. M. Ding, F. S. He, X. Y. Yu, J. Zhou, Y. J. Hu and J. W. Xie, *Langmuir*, 2008, **24**, 1026.
3 G. Zhang, Y. Gao, Y. Zhang and Y. Guo, *Environ. Sci. Technol.*, 2010, **44**, 6384.
4 P. Aranda, R. Kun, M. Angeles Martín-Luengo, S. Letaïef, I. Dékány and E. Ruiz-Hitzky, *Chem. Mater.*, 2008, **20**, 84.
5 A. Rodríguez, G. Ovejero, M. Mestanza and J. García, *Ind. Eng. Chem. Res.*, 2010, **49**, 3207.
6 J. Liu, D. Mengqin, Z. Shengli and Y. Yingchun, *Appl. Clay Sci.*, 2009, **43**, 156.
7 C. Li, J. Wang, S. Feng and Z. Liu, *Chin. J. Chem.,* 2014, **32**, 599.
8 S. Barrientos-Ramírez, E. V. Ramos-Fernández, J. Silvestre-Albero, A. Sepúlveda-Escribano, M. M. Pastor-Blas and A. González-Montiel, *Microporous Mesoporous Mater.*, 2009, **120**, 132.
9 E. Abdullayev, K. Sakakibara, K. Okamoto, W. Wey, K. Ariga and Y. Lvov, *ACS Appl. Mater. Interfaces*, 2011, **3**, 4040.
10 L. Wang, J. Chen, L. Ge, Z. Zhu and V. Rudolph, *Energy Fuels*, 2011, **25**, 3408.
11 J. Liang, B. Dong, S. Ding, C. Li, B. Q. Li, J. Li and G. Yang, *J. Mater. Chem. A*, 2014, **2**, 11299.
12 C. Li, J. Wang, X.Luo and S. Ding, *J. Colloid Interface Sci.*, 2014, **420**, 1.
13 P. Yuan, P. D. Southon, Z. Liu, M. E. R. Green, J. M. Hook, S. J. Antill and C. J. Kepert, *J. Phys. Chem. C*, 2008, **112**, 15742.
14 C. Li, J. Liu, X. Qu, B. Guo and Z. Yang, *J. Appl. Polym. Sci.*, 2008, **110**, 3638.
15 W. O. Yah, A. Takahara and Y. M. Lvov, *J. Am. Chem. Soc.*, 2012, **134**, 1853.
16 G. Cavallaro, G. Lazzara and S. Milioto, *Langmuir*, 2011, **27**, 1158.
17 V. Vergaro, E. Abdullayev, Y. M. Lvov, A. Zeitoun, R. Cingolani, R. Rinaldi and S. Leporatti, *Biomacromolecules*, 2010, **11**, 820.
18 B. Wu, H. H. Hng and X. W. Lou, *Adv. Mater.*, 2012, **24**, 2567.
19 J. Zhang, Q. Xu, Z. Feng, M. Li and C. Li, *Angew. Chem., Int. Ed.*, 2008, **120**, 1790.
20 Y. Liao, W. Que, Q. Jia, Y. He, J. Zhang and P. Zhong, *J. Mater. Chem.*, 2012, **22**, 7937.
21 R. Asahi, T. Morikawa, T. Ohwaki and K. Aoki, Y. Taga, *Science*, 2001, **293**, 269.
22 Q. Dong, H. Yu, Z. Jiao, G. Lu and Y. Bi, *RSC Adv.*, 2014, **4**, 59114.
23 J. Tang, D. Li, Z. Feng, Z. Tan and B. Ou, *RSC Adv.*, 2014, **4**, 2151.
24 C. Xue, T. Wang, G. Yang, B. Yang and S. Ding, *J. Mater. Chem. A*, 2014, **2**, 7674.
25 H. Zhang, R. Zong, J. Zhao, Y. Zhu, *Environ. Sci. Technol.*, 2008, **42**, 3803.
26 E. T. Kang, K. G. Neoh and K. L. Tan, *Prog. Polym. Sci.*, 1998, **23**, 211.
27 Y. Zhu, D. Hu, M. X. Wan , L. Jiang and Y. Wei, *Adv. Mater.*, 2007, **21**, 2092.
28 R. Ramakrishnan, J. D. Sudha and V. L. Reena, *RSC Advances*, 2012, **2**, 6228.
29 M. A. Salem, A. F. Al-Ghonemiy and A. B. Zaki, *Appl. Catal., B*, 2009, **91**, 59.
30 S. Min, F. Wang and Y. Han, *J. Mater. Sci.*, 2007, **42**, 9966.
31 H. Ma, Y. Li, S. Yang, F. Cao, J. Gong and Y. Deng, *J. Phys. Chem. C*, 2010, **114**, 9264.
32 O. Abdulrazzaq, S. Bourdo, V. Saini, V. G. Bairi, E. Dervishi,T. Viswanathan, Z. A. Nima and A. S. Biris, *Energy Technol.*, 2013, **1**, 463.
33 C. Li, J. Wang, H. Guo and S. Ding, *J. Colloid Interface Sci.*, 2015, **458**, 1.
34 D. Papoulis, S. Komarneni, A. Nikolopoulou, P. Tsolis-Katagas, D. Panagiotaras, H. G. Kacandes, P. Zhang, S. Yin, T. Sato and H. Katsuki, *Appl. Clay Sci.*, 2010, **50**, 118.
35 D. Papoulisa, S. Komarneni, D. Panagiotaras, E. Stathatos, D. Toli, K. C. Christoforidis, M. Fernández-Garciae, H. Li, S. Yin, T. Sato and H. Katsuki, *Appl. Catal., B*, 2013, **132**, 416.
36 C. Li, J. Wang, S. Feng, Z.Yang and S. Ding, *J. Mater. Chem. A*, 2013, **1**, 8045.
37 E. A. Barringer and H. K. Bowen, *Langmuir*, 1985, **1**, 420.
38 Z. Niu, Z. Yang, Z. Hu, Y. Lu and C. C. Han, *Adv. Funct. Mater.* 2003, **13**, 949.
39 J. E. Albuquerque, L. H. C. Mattoso, D. T. Balogh, R. M. Faria, J. G. Masters and A. G. MacDiarmid, *Synth. Met.* 2000, **113**, 19.

Graphical Abstract

One-dimensional heterogeneous polyaniline-crystalline TiO_2-halloysite nanotubes with enhanced visible-light photocatalytic activity were achieved by tuning the acid dopant in the preparation at low temperature